Solid State Phenomena Vol. 105 (2005) pp. 291-296
online at http://www.scientific.net

Texture development in Nd-Fe-V and Nd-Fe-B alloys by hot forging in view of improving permanent magnet properties

S. Rivoirard[1,a], I.Popa[2,b] , D. Chateigner[3,c], B. Ouladdiaf[4,d], P. de Rango[2,e], D. Fruchart[2,f]

[1] CRETA-CNRS, BP 166, 38042 Grenoble, France

[2] Laboratoire de Cristallographie-CNRS, BP 166, 38042 Grenoble, France

[3] CRISMAT-ENSICAEN, 6, boulevard du Maréchal Juin, 14050 Caen, France

[4] Institut Laue Langevin, 6 Rue J. Horowitz, BP 156, 38042 Grenoble, cedex 9, France

[a]sophie.rivoirard@grenoble.cnrs.fr, [b]ioana.popa@grenoble.cnrs.fr, [c]daniel.chateigner@ismra.fr, [d]ouladdiaf@ill.fr,[e]derango@grenoble.cnrs.fr, [f]daniel.fruchart@grenoble.cnrs.fr

Keywords: $Nd_2Fe_{14}B$ phase, $Nd(Fe,V)_{12}$ phase, texture, hot forging, permanent magnet.

Abstract. A high speed hot forging process was applied to Nd-Fe-B and Nd-Fe-V as cast alloys in order to develop both the microstructure and the crystallographic texture appropriate for permanent anisotropic magnet properties. Neutron diffraction texture analyses are used to demonstrate the effect of the hot forging process on both kind of alloys. Microstructural changes are an important feature on forging in both cases. Coercivity is developed in the Nd-Fe-B alloy mainly from grain size reduction and disappearance of free iron. Stabilisation of the $Nd(Fe,V)_{12}$ hard magnetic phase is achieved from the iron and Nd-rich microstructure of the starting Nd-Fe-V material. A comparison of the crystallographic textures of $Nd_2Fe_{14}B$ and $Nd(Fe,V)_{12}$ phases is done to account for the development of extrinsic magnetic anisotropy. In both cases, a nearly fibre texture is obtained in correlation with the symmetry of the deformation. However, the orientations are quite different in both alloys and the consequences on the magnetic properties are evidenced.

Introduction

In the field of bonded magnets, very large energy products are now one of the major concerns of applied research. Bonded magnets may be obtained by mixing a permanent magnet powder within a polymer. As a result of the crystallite random orientation, the magnetization remanence, $\mu_0 M_r$, is generally below 0.8T. The production of textured materials is thus indispensable in view of obtaining magnets with higher energy products. Several routes have been explored with this aim [1-3]. Anisotropic Nd-Fe-B powders are already commercially available in small quantities from various but costly processes (HDDR process or mechanical deformation of melt-spun ribbons followed by grinding) whereas, only recently some studies report on Nd-Fe-V-N alloys with potential permanent magnet properties [4]. In this study, we propose to apply the combined high-speed bulk forging and HD process [5] to the development of permanent magnet properties in Nd-Fe-B and Nd-Fe-V alloys. In the case of Nd-Fe-B alloys, the hard magnetic phase is the well known tetragonal $Nd_2Fe_{14}B$ phase ($P4_2/mnm$) with a saturation magnetization of 1,5 T, an anisotropy field of 7 T and a Curie temperature of 315°C. Anisotropic Nd-Fe-B-Cu powders have already been obtained with the combined hot forging and HD process (H_c=10 kOe, B_r=1 T, BH_{max}=200 kJ/m^3) [2]. The $NdFe_{12-X}V_X$ compounds of $ThMn_{12}$-type structure (I4/mmm) can be considered as potential permanent magnet materials because of their high magnetization level. Moreover their Curie temperatures and magnetocrystalline anisotropies are drastically increased by insertion of interstitial elements [6]. For instance, the $NdFe_{10,5}V_{1,5}N$ compound has a Curie temperature of 510°C and an anisotropy field of 11 T (higher than the $Nd_2Fe_{14}B$ phase). Therefore, the preparation route of a $NdFe_{10,5}V_{1,5}N$ type magnet powder will include a third step of nitrogenation after the hot forging and HD processes.

Experimental details

Samples of the $NdFe_{10.5}V_{1.5}$ composition with a Nd-excess of 3, 10, 15 and 20% and $NdyFe_{93.5-y}B_5Cu_{1.5}$ alloys with y = 12, 15.5, 17 and 20 were prepared by induction melting and were cast into cylindrical stainless steel tubes of 12 mm in diameter. The high speed hot forging process was then applied on these ingots under argon atmosphere at 930°C for the Nd-Fe-V alloys and 980°C for the Nd-Fe-B-Cu alloys. The forging direction, Y, was parallel to the cylinder axis of the ingot. The deformation rate reached $100s^{-1}$. The Nd-Fe-V alloys and the Nd-Fe-B-Cu alloys present close microstructures. Both are composed of two main phases. The hard magnetic phase ($NdFe_{10.5}V_{1.5}$ and $Nd_2Fe_{14}B$ respectively) is solid at the forging temperature, T_f. The intergranular neodymium-rich phase is non magnetic and is liquid above 785 K. The samples were then studied by scanning electron microscopy and the images analyzed using Scion Image. Neutron diffraction experiments have been performed at ILL, Grenoble, on the D1B beamline (λ = 2,532 Å) for Nd-Fe-B and on the D20 diffractometer (λ = 1.3 Å) for Nd-Fe-V, using Eulerian cradles and curved position sensitive detectors. The data treatment was operated using XRFIT (developed at ILL), POFINT [7], GOMAN [8] and Beartex [9]. In this study, the results on $Nd_{15,5}Fe_{78}B_5Cu_{1.5}$ were aimed to test the influence of free iron on the texturing mechanism. Therefore the measurements were run on two samples of the same forged ingot extracted from two areas where the residual iron content was different: the center and the periphery. As two φ-scans (at χ=0° and 90°) revealed an axially symmetric texture for Nd-Fe-B, only χ-scans were measured.For $NdFe_{10.5}V_{1.5}$ +3% Nd and $NdFe_{10.5}V_{1.5}$ +10% Nd forged samples, χ-scans from 0° to 90° and φ-scans from 0° to 355° (5° steps) were measured.

Results

Microstructure and coercivity. For both Nd-Fe-B-Cu and Nd-Fe-V, microstructure changes are very important during the forging step. For the $Nd_{15.5}Fe_{78}B_5Cu_{1.5}$ and $NdFe_{10.5}V_{1.5}$+10%at Nd optimized compositions, the difference between the as-cast state (Fig. 1a and 1c) and the as-forged state is very marked (Fig. 1b and 1d). For Nd-Fe-B-Cu, free iron dendrites are numerous and centered in $Nd_2Fe_{14}B$ grains (as primary nuclei) in the as cast state. The $Nd_2Fe_{14}B$ grains have a platelet like shape. The $Nd_2Fe_{14}B$ grain size and the intergranular phase distribution are not homogeneous. In the forged state, the microstructure is well refined. The $Nd_2Fe_{14}B$ grains are equiaxed. The intergranular phase is homogeneously distributed around the hard magnetic grains supplying thus a magnetic decoupling suitable for coercivity. Free iron is scarce (less than 1-% volume fraction). The $Nd_2Fe_{14}B$ grain size has been reduced to a few microns by cracking. This fracture process occurring on forging enables the Nd-rich liquid phase to get in contact with iron through the cracks and to dissolve it. This results in an iron enrichment of the intergranular phase and the disappearance of the soft ferromagnetic iron phase. The forged alloy presents a coercivity of 10 kOe. Contrary to NdFeB, as cast NdFeV does not contain the hard magnetic $NdFe_{10.5}V_{1.5}$ phase. Before forging, the samples are all composed of a mixture of Fe-V dendrites and a Nd-rich intergranular phase ; the $Nd(Fe,V)_{12}$ phase can not be observed. The application of the high speed hot forging process allows the stabilization of $Nd(Fe,V)_{12}$ and the almost complete dissolution of iron. This forging step revealed equivalent to a long annealing treatment (24 hours at 950°C or one week at 900°C). This $NdFe_{10.5}V_{1.5}$+10%at Nd sample presents less than 5% of free iron and a homogeneous 5% content of intergranular phase. The $Nd(Fe,V)_{12}$ phase has a grain size of about 10µm. In term of coercivity, the microstructure obtained on this sample is almost convenient. Even if grain refinement did not proved to be as efficient as compared to the $Nd_2Fe_{14}B$ phase, the hard magnetic $Nd(Fe,V)_{12}$ phase is stabilised and surrounded with a fine coating of the Nd-rich intergranular phase. However, no coercivity was obtained after nitriding the 200 microns powders, but maybe for nitriding reasons [10].

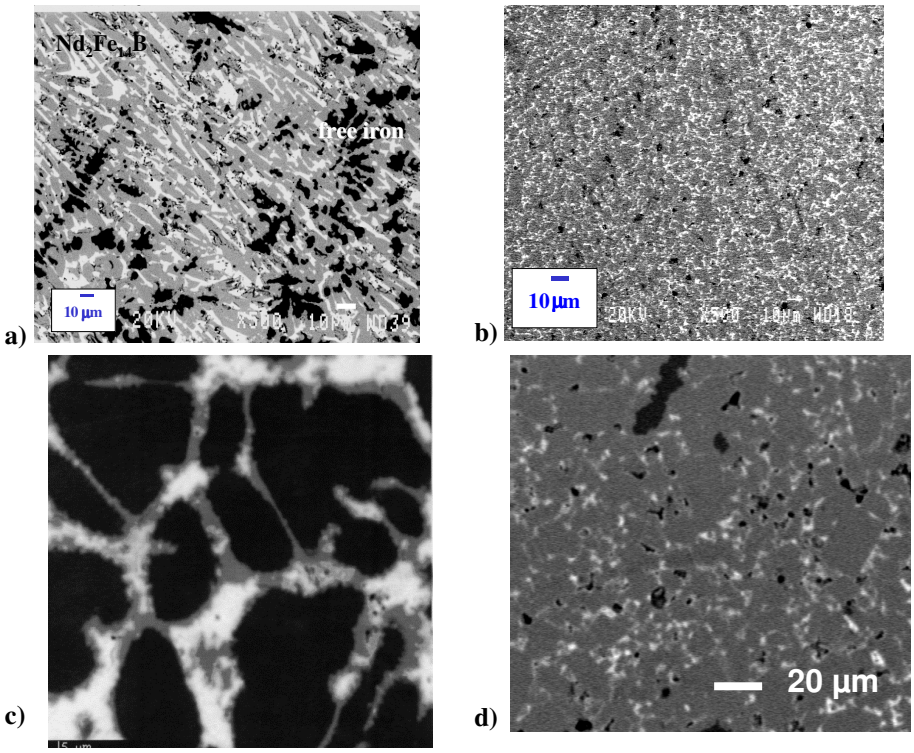

Figure 1: SEM micrographs of the $Nd_{15.5}Fe_{78}B_5Cu_{1.5}$ alloy a) before and b) after forging and of the $NdFe_{10.5}V_{1.5}$+10%at Nd alloy c) before and d) after forging. Black: iron, grey: hard magnetic phase ($Nd_2Fe_{14}B$ or $Nd(Fe,V)_{12}$), white: Nd-rich phase.

Texture development. Extrinsic magnetic anisotropy can be developed through the crystallographic texture. For $Nd_2Fe_{14}B$ and $Nd(Fe,V)_{12}N$, the c-axis of the structure is the magnetization easy axis. Therefore, alignment of the crystallite c-axes should optimize the magnetization in one direction. $Nd_{15.5}Fe_{78}B_5Cu_{1.5}$ samples showed the development, on forging, of a fiber texture of $Nd_2Fe_{14}B$, suitable for extrinsic magnetic anisotropy [11]. Only <001> axes were aligned parallel to Y. With this configuration, remanence is enhanced in the forging direction, and reduced perpendicularly. In both $NdFe_{10.5}V_{1.5}$ +3% Nd and $NdFe_{10.5}V_{1.5}$ +10% Nd forged samples, as shown on Fig. 2, a nearly fiber texture was observed with the <100> directions parallel to Y. This texture however shows two slight components around Y. The texture is weaker than in the NdFeB sample, with volume fractions of randomly oriented grains near 70 % in $NdFe_{10.5}V_{1.5}$ +10% Nd and only 36% in $NdFe_{10.5}V_{1.5}$ +3% Nd. The {001} pole figure shows the nearly random orientation of the <001> (c-axis) of the crystallites around <100> with two slight reinforcements. This configuration is not convenient for extrinsic magnetic anisotropy, particularly with the high volume fraction of randomly oriented crystallites.

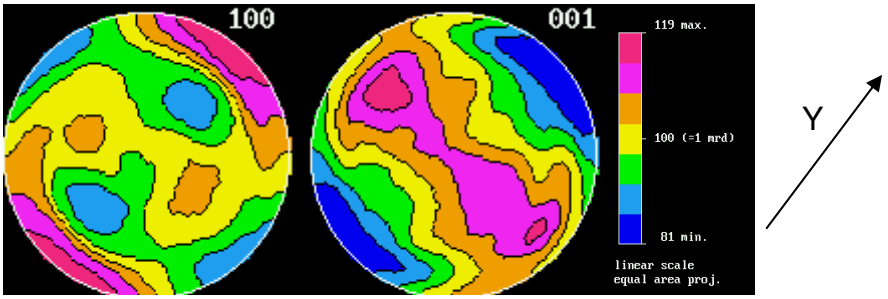

Figure 2: {100} and {001} WIMV-recalculated pole figures of the forged sample (Y= forging direction).

Influence of the starting microstructure on texturing. The texturing process of the hard magnetic main phase is strongly influenced by the ensemble rheology and thus by minor phases contribution (intergranular phase and iron). As shown on Fig. 3, the amount of liquid phase at the forging temperature is linked to the composition in Nd of the starting alloy. Liquid volume fractions linearly increase with Nd. For Nd-Fe-B-Cu, this linear behavior remained in the forged samples, to a lower volume fraction of intergranular phase after $Nd_2Fe_{14}B$ formation.

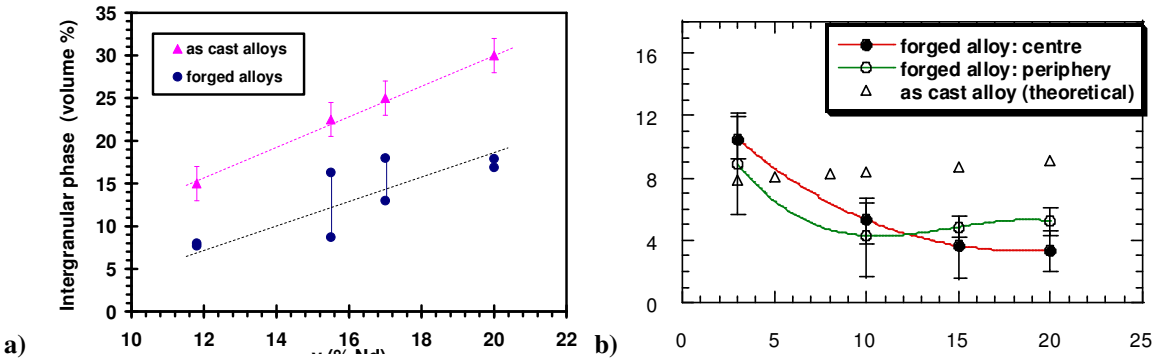

Figure 3: intergranular phase volume fraction as a function of neodymium content (in %) in the starting alloy and in the forged sample for a) Nd-Fe-B-Cu and b) Nd-Fe-V.

Concerning Nd-Fe-V, the major part of the Nd-rich phase reacts with iron to form the $NdFe_{10.5}V_{1.5}$ phase during the forging step. Fig. 3 shows a decrease of the intergranular phase when the Nd content increases. This can be related to a more efficient recombination of Nd with Fe for higher intergranular phase fraction (Fig. 4). However, for larger Nd contents, nucleation of the $NdFe_{10.5}V_{1.5}$ phase is no longer efficient. An important amount of liquid phase is rejected to the periphery of the sample and do not react, thus leading to an increase in residual iron amount. The optimum (near 90% of $NdFe_{10.5}V_{1.5}$ phase) condition is for 10% Nd in excess.

The presence of free iron in the starting materials is not detrimental to the deformation behaviour and to the texturing step. As can be seen on Fig. 5, for Nd-Fe-B-Cu, the best permanent magnet properties and the lowest amount of residual iron are obtained in the sample with the initially highest volume fraction of free iron (y = 15,5%). This case corresponds to an optimized phase transformation with the highest amount of hard magnetic phase (around 90% of $Nd_2Fe_{14}B$) and a good intergranular phase distribution.

In the $NdFe_{10.5}V_{1.5}$ +10% Nd sample, the $NdFe_{10.5}V_{1.5}$ phase is properly stabilized from a starting microstructure of *only* free iron and the Nd-rich phase, and its texture is developed.

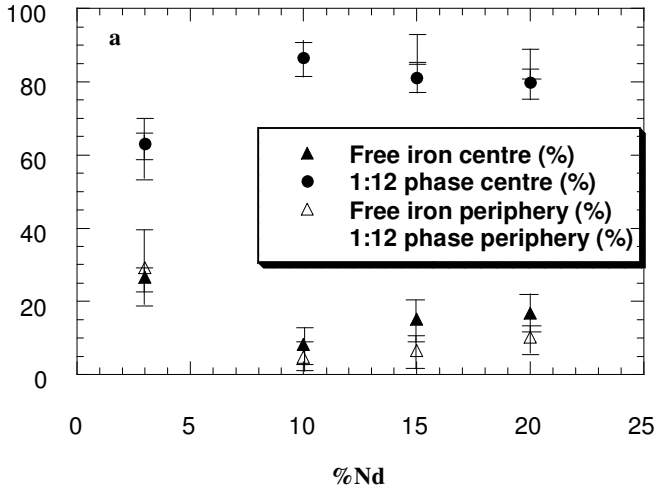

Figure 4: 1:12 intergranular and free Fe phase contents for the samples forged at 930°C, in the center and at periphery of the cylinder.

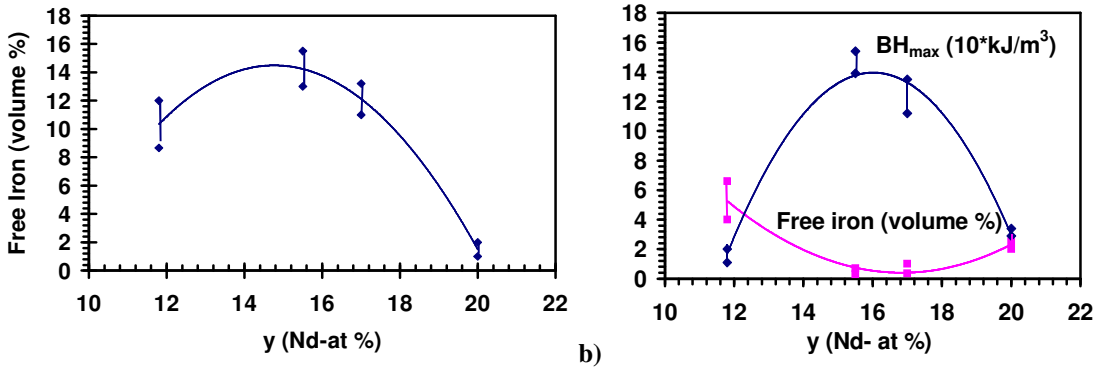

Figure 5: Free iron volume fraction in $Nd_yFe_{93.5-y}B_5Cu_{1.5}$ versus Nd content for a) as-cast alloys and b) forged alloys. Correlation with the energy product of the corresponding forged magnets.

In order to clarify the influence of iron on the deformation behavior, the texture of two Nd-Fe-B-Cu samples taken from the same forged specimen were analyzed. The sample taken from the periphery contained large iron aggregates before forging, while the center sample showed rather homogeneous iron dendrites. A SEM picture of the peripheric sample and the (002) pole density variations for each sample are presented on Fig. 6. Again, the same fiber texture of $Nd_2Fe_{14}B$ (<001> axes aligned parallel to Y) was recorded in both samples. However, a weaker texture (1.2 mrd at maximum) was observed in the region containing the primary iron aggregates. Moreover, after forging, the microstructure of this region consists of two different aspects: (i) refined $Nd_2Fe_{14}B$ grains and well distributed intergranular phase for the regions where the $Nd_2Fe_{14}B$ grains are *not* connected to residual iron and (ii) poor refinement and phase distribution in areas where iron dendrites are absent. As can be seen from this image, grains connected to an iron dendrite did not undergo any deformation and thus any texturation. This dual microstructure can explain the weak (002) pole density: the <001> fiber texture emerges from the deformed region (i) whereas the weak texture can be accounted for the high volume fraction of non-deformed, randomly oriented grains (ii). Thus, outside the optimized rheological conditions, iron is responsible of the weak deformation and bad texturing of the main phase.

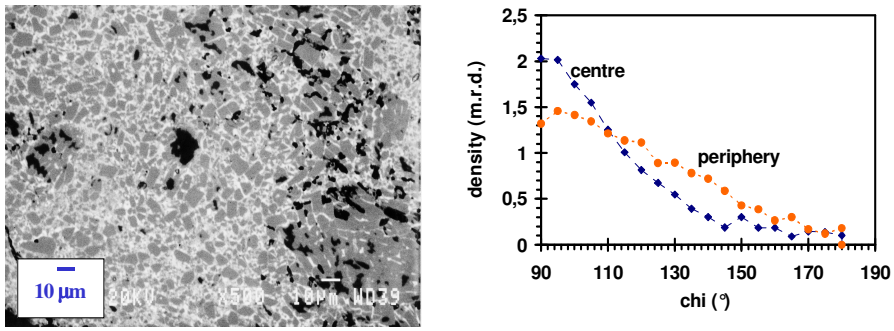

Figure 6: a) SEM micrographs of the periphery of a forged sample: (black: iron aggregates) and b) (002) pole density variation for the center and periphery of a forged magnet (respectively without and with free iron aggregates).

SEM observations of Fig.7 were done on a $Nd_{12}Fe_{81,5}B_5Cu_{1.5}$ forged sample, far from the optimized composition to understand how the presence of iron can hinder the texturing process in some cases. This sample did not present any extrinsic anisotropy. A large amount of iron was still present in this sample after forging. Moreover, we observed the plastic deformation of iron dendrites in the direction perpendicular to the forging direction. A similar deformation was obtained on Nd-Fe-V samples for low forging temperature [10].

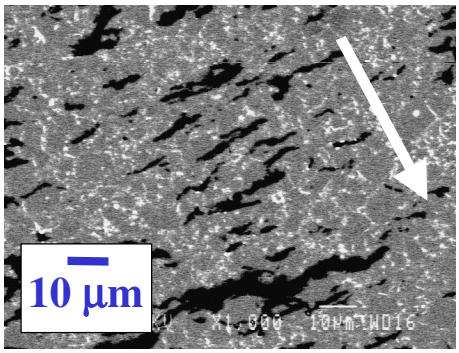

Figure 7: SEM image parallel to the forging direction (arrow) of a) forged $Nd_{12}Fe_{81,5}B_5Cu_{1.5}$ sample exhibiting plastic deformation of Fe.

Discussion and Summary

It is surprising that two alloys like Nd-Fe-B and Nd-Fe-V with similar microstructures may have such different deformation behaviors. During the high speed forging step, both $Nd_2Fe_{14}B$ and $Nd(Fe,V)_{12}$ phases are probably in a brittle state [2]. The fiber texture in both $Nd_2Fe_{14}B$ and $Nd(Fe,V)_{12}$ can be explained by the uniaxial symmetry of the deformation process (forging). But as compared to the convenient c-axis fiber texture of the $Nd_2Fe_{14}B$ phase, the $Nd(Fe,V)_{12}$ texture with a-axes // Y was not expected. It results from this study that even minor phases can have a large influence on the deformation behavior of the alloy, i.e. the intergranular phase. In Nd-Fe-B, high liquid volume fractions (>15%) make the deformation a semi-solid state process. In Nd-Fe-V alloys, the lower amount of liquid phase (in optimized conditions) induces a quasi solid deformation process. In non-optimized conditions, iron plasticity can accommodate deformation at the expense of the hard magnetic phase deformation and texturing. In the semi-solid state, a global $Nd_2Fe_{14}B$ particle flow occurs on the liquid simultaneously with $Nd_2Fe_{14}B$ crystallites rotation and fracture leading to the best permanent magnet properties (BH_{max}=200 kJ/m^3). Concerning Nd-Fe-V, the texturing mechanism involves the low liquid volume fraction (<5% in volume) which blocks grain rotations at the forging temperature, explaining a larger random component for larger Nd-excess values.

References

[1] C. Mishima, N. Hamada, H. Mitarai, Y. Honkura: Proc. of the 16th International Workshop on Rare-Earth magnets and their Applications, Sendai (2000), p.873.
[2] S. Rivoirard, P. de Rango, D. Fruchart, Y. Chastel, and C. Martin: Material Science and Engineering A 311(1-2) (2001), p. 121-127.
[3] G.P. Meisner, V. Panchanathan: J. Appl. Phys. 76 (10) (1994), p. 6259.
[4] S.L. Tang, C.H. Wu, X.M. Jin, B.W. Wang, G.S. Li, B.Z. Ding, Y.C. Chuang: J.Magn.Magn.Mater. 189 (1998), p.202.
[5] S. Rivoirard, P. de Rango, D. Furchart, R. Perrier de la Bâthie : patent n° 98 06745 (1998).
[6] B.P. Hu, Y.Z. Wang, K.Y. Wang, G.C. Liu, W.Y. Lai: J. Magn.Magn.Mater. 140-144 (1995), p.1023.
[7] D. Chateigner, *"Pofint, exploitation directe des figures de pôles"*, licence L03084, CRISMAT/INEL (2003).
[8] D. Chateigner, H. Pillière, programme INEL/CRISMAT (1999).
[9] H.R. Wenk, S. Matthies, J. Donovan, D. Chateigner: J. Appl. Cryst. 31 (1998), p.262-269.
[10] I. Popa, Ph. D. Thesis, Université J. Fourier, Grenoble, France (2003).
[11] S. Rivoirard, D. Chateigner, P. De Rango, D. Fruchart: Mater. Science Forum vols 402-412 (2002), p.173-178.